Nb$_3$Sn FILMS FOR SRF CAVITIES: GENESIS AND RF PROPERTIES*

U. Pudasaini[1], G. V. Eremeev[2], C. E. Reece[2], J. Angle[3], J. Tuggle[3], M. J. Kelley[1, 2, 3]

[1]Applied Science Department, The College of William and Mary, Williamsburg, VA 23185, USA
[2]Thomas Jefferson National Accelerator Facility, Newport News, VA 23606, USA
[3]Virginia Polytechnic Institute and State University, Blacksburg, VA 24061, USA

Abstract

Understanding of Nb$_3$Sn nucleation and growth is essential to the progress with Nb$_3$Sn vapor diffusion coatings of SRF cavities. Samples representing different stages of Nb$_3$Sn formation have been produced and examined to elucidate the effects of nucleation, growth, process conditions, and impurities. Nb$_3$Sn films from few hundreds of nm up to ~15 μm were grown and characterized using AFM, SEM/EDS, XPS, EBSD, SIMS, and SAM. Microscopic examinations of samples suggest the mechanisms behind Nb$_3$Sn thin film nucleation and growth. RF measurements of coated cavities were combined with material characterization of witness samples to adapt the coating process in "Siemens" coating configuration. Understanding obtained from sample studies, applied to cavities, resulted in Nb$_3$Sn cavity with quality factor 2×10^{10} at 15 MV/m accelerating gradient at 4 K, without "Wuppertal" Q-slope. We discuss the genesis of the Nb$_3$Sn thin film in a typical tin vapor diffusion process, and its consequences to the coating of SRF cavities.

INTRODUCTION

Discovered in 1954 by Bernd Matthias [1], Nb$_3$Sn is a promising alternative material to replace niobium for SRF cavities. Its critical temperature (~ 18 K) and predicted superheating field (~ 400 mT) are nearly twice those of niobium, thereby promises the possibility of attaining higher quality factor and accelerating gradient at any given temperature [2]. It can also allow an increase of the cavity operation temperature from 2 K to 4 K to reduce both capital and operating cost significantly. However, lower thermal conductivity and brittleness of Nb$_3$Sn limits its application to thin film/coating form. Nb$_3$Sn thin films should be deposited inside built-in metallic (e.g. Nb, Cu) cavity structure. Since SRF cavities typically have complicated geometries, and demands uniform coating, suitable thin film deposition techniques are restricted. Among several techniques attempted to deposit Nb$_3$Sn thin films, vapor diffusion coating is the most favorable and successful technique so far.

Vapor diffusion coating of Nb$_3$Sn on niobium cavities dates back to 1970's [3-5]. This technique is adopted recently by several research institutions develop Nb$_3$Sn coated cavities [6-9]. Recent performance results of such cavities are very promising by attaining high quality factors, $> 10^{10}$ operating at 4.2 K at medium fields at ≥ 15 MV/m in several labs. The essence of vapor diffusion technique is to deliver tin vapor to the niobium at high temperature environment, normally at 1100-1200 ºC. According to Nb-Sn binary phase diagram, the Nb$_3$Sn phase forms exclusively at temperature > 930 ºC [10].

Attributed to Saur and Wurm [11], vapor diffusion technique was first employed in Siemens AG to deposit Nb$_3$Sn films for SRF applications. The technique was then adopted by Kernforschungszentrum Karlsruhe (KfK), Wuppertal University and Cornell Universities in 1970's. Significant research and development work was done in Wuppertal to refine the deposition technique, which was then transferred as a *"recipe"*. The vapor diffusion process in practice at several labs follow Siemen AG or Wuppertal coating protocols with some modifications. Wuppertal-like systems are equipped with a secondary heater to control the temperature of the Sn-source independently. Siemens-like coating systems are single heater system. While application of Nb$_3$Sn films is so promising and has a long history, only limited research are available addressing the growth of Nb$_3$Sn thin film during the vapor diffusion process, explicitly used to coat SRF cavities. The quality of coated Nb$_3$Sn layers is contingent on understanding coating layer formation and growth during the process.

To elucidate the Nb$_3$Sn film growth during the deposition process, samples were coated with various coating variables, and studied them with several material characterization techniques. Several witness samples were also coated with SRF cavities to assess process parameters. In this paper, we will discuss the genesis of Nb$_3$Sn thin film in a typical vapor diffusion technique used to coat SRF Nb cavities including RF results from coated cavities.

Nb$_3$Sn THIN FILM DEPOSITION

Nb$_3$Sn thin film deposition at JLab consists 99.999% or better purity tin and 99.99% tin chloride powder, both purchased from Sigma Aldrich or American Elements, which are placed at the bottom of the sample chamber or SRF cavity made of niobium (RRR~300). Samples are mounted inside the chamber and both sides are closed with Nb foil or Nb covers. The setup assembled in the cleanroom is then transported to Nb$_3$Sn deposition system in the thin film lab. The deposition system is comprised of two parts: the furnace, to provide a clean heating environment, and the insert, made of niobium, inside which the experimental setup is loaded for each experiment. The coating setup is installed into the insert and evacuated. Once the insert pressure reaches $\leq 10^{-5}$ Torr range, the

heating profile is initiated. It comprises of two-steps: nucleation-then-growth sequence. The first temperature plateau at 500 ºC is dedicated to the nucleation process and the second at 1200 ºC facilitates coating growth, see Fig. 1. Cavity coating normally uses the similar temperature profile.
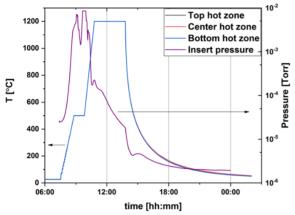

Figure 1: Temperature profile used for coating Nb_3Sn on niobium samples at Jlab. Temperature of the insert during the process is monitored with three themocouples at different sections of the insert. Because of very similar temperature readings, the temperature curves are overlapped.

Several sets of experiments were run to get an insight on coating genesis during the process. The coating process was interrupted at different stages to observe the evolution of Nb_3Sn thin films. Several samples were produced by varying the nucleation parameters during the nucleation studies. A set of experiments were run to determine the effects of different coating parameters. Several samples were coated for different coating times and temperatures. To understand the coating growth mechanism, a set of "*overcoat*" experiments were designed. Samples were systematically coated with Nb_3Sn under conditions, where a number of Nb_3Sn samples were subjected to coating over several times for different durations. Witness samples were coated and studied with cavities to correlate coating characteristics with RF performances.

NUCLEATION

Following the nucleation step at 500 ºC for an hour, all the $SnCl_2$ was evaporated. Tin vapour pressure at this temperature is low and can be ignored. Secondary electron microscopy (SEM) examination of nucleated samples showed sub-micron sized spherical particles, appearing as bright features in SEM image shown in Fig. 2. Spherical particles were examined with energy-dispersive X-ray spectroscopies (EDS), showed 40-70 at. % Sn depending on size indicating to be tin particles. Larger particles showed more tin, as would be expected, since the spatial resolution limit of EDS is larger than the particle size. Therefore the data from individual particles included more or less Nb signal as well from adjacent or underlying material. EDS was unable to detect any tin in between

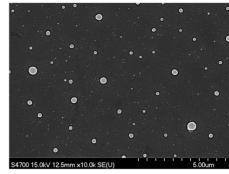those particles. Surface coverage of those particles was < 5 %.

Figure 2: SEM image obtained from sample coated at 500 ºC for one hour. Note that the circular bright features are Sn.

Further analysis of similar samples with XPS resulted in ~ 30% total tin. Note that the XPS signal is obtained from only few nanometer of a top surface. This discrepancy of tin content between SEM and XPS analysis indicated the presence of more tin than the particles visible in SEM. To gain more insight, similar samples were examined with scanning auger microscopy (SAM), which has ability collect auger electrons for elemental analysis, and map it to corresponding SEM image. Elemental mapping of Sn corresponding to an SEM image is shown in Fig. 3. Large bright features, consistent with Sn particles seen in the SEM, like Fig. 3 show expectedly high tin content. The intervening area between Sn particles also shows the presence of tin. Transmission electron microscopy (TEM) was used to examine cross-section of a nucleated sample, treated at 500 °C for 5 hours. TEM- EDS line scans, not shown here were then obtained passing through and away from the particles in the cross-section. An EDS line scan passing of an area away from Sn particles also showed tin and oxygen signal close to the surface indicating the presence additional tin in between visible tin particle in SEM. Niobium substrate evidently develops Sn particles and ultra-thin Sn film at the surface following the nucleation. Nucleation parameter variation could result in drastically different surfaces following nucleation, but mostly with ultra-thin film of Sn. More details are available in [12].
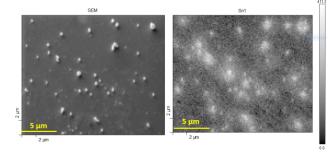

Figure 3: SAM elemental mapping of Sn coverage after sputtering for thirty seconds is shown in the image (lower left). The brighter areas are richer in Sn than darker area as shown in intensity scale.

GROWTH

Following the nucleation at 500 °C, temperature is ramped at the rate of 12 °C per minute to reach the coating temperature. Tin starts to evaporate and reacts with niobium which readily deposits Nb_3Sn thin film, even before the coating temperature is attained. Figure 4 (a) shows an SEM image obtained from a sample, coated for 5 minutes at 1200 °C, which shows the uniform coverage of Nb_3Sn coating. The grain sizes are on the order of few tens of nanometers at this point. It has been found that, the coatings are often susceptible to non-uniformity in absence of $SnCl_2$, as shown in Figure 4 (b). These patchy regions were also seen after 3 hours of longer coating. Note patch-free coatings have been observed without $SnCl_2$ in a few experiments which was linked to higher amounts of tin evaporation with provided larger surface area of tin source. Grain size grows swiftly with longer coating. For the same set of coating parameters used to produce 4 (a), the grain size was few hundreds of nanometers after an hour and about one micron with complete coating of 3 hours.
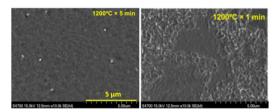

Figure 4: SEM images obtained from coated samples with [left] and without [right] $SnCl_2$, soon after reaching the coating temperature [13].

After the first layer of Nb_3Sn is established on the surface, further growth of Nb_3Sn requires the mobility of Sn or Nb through Nb_3Sn thin film. To understand the growth mechanism of Nb_3Sn during a coating step, a set of standard niobium samples were coated for 1 hour at 1200 °C. After the run, several samples were removed, and the remaining samples with added new niobium samples were then coated, "*overcoated*", again for 1 hour without SnCl2. The overcoat procedure was repeated for 1, 1, 3, 12 and 60 hour respectively in successive coating runs. The total cumulative coating time varied from 1 hour to 78 hours. The supplied amount of Sn was always more than it consumed in each experiment. A set of SEM images, seen in Figure 5, were obtained from sequentially overcoated samples and show microstructure evolution. EDS examination showed (24 ± 0.5) at. % Sn without any notable changes in surface composition following each overcoat. Average grain sizes were estimated for both the single-coat and overcoat samples from each coating run of the sequential overcoat series. Several SEM images were captured from each sample with magnifications where grains were distinctly visible. 4-6 lines were drawn along the length over each image, and the number of intersections between the lines and grain boundaries were manually counted. The average grain size was determined as the average distance between intersections. The average grain size was found to increase following each overcoat, and

varied between 1.6 to 6.6 µm as shown in Figure 6. The average grain size was found to follow power law dependence with total coating time,

$$z = (1.53 \pm 0.06)t^{0.34 \pm 0.01} \qquad (1)$$

Where z and t are grain size (µm) and time (hour) respectively.

Coating cross-sections from each overcoat run were examined by XPS sputter depth profiles, electron backscatter diffraction (EBSD), and optical microscope. XPS sputter depth profiles, not shown here, showed that the tin concentration from the surface to Nb_3Sn-Nb interface were similar in different overcoats, and qualitatively resembles XPS depth profiles from single coat samples. A near constant tin composition exists from surface through the thickness of the coating, and ends with steady drop near Nb_3Sn-Nb interface. The thickness of the coating increased after each overcoat. The depth of near constant tin concentration close to the surface increased with each overcoat.   Similarly, the depth over which tin dropped at Nb_3Sn-Nb interface increased with each overcoat.
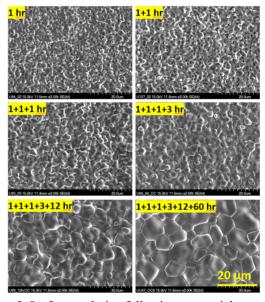

Figure 5: Surface evolution following sequential overcoats. Note that images are captured at same magnification
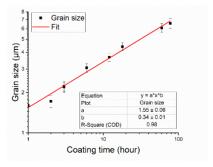

Figure 6: Average grain size variation with total coating time.

EBSD data on samples coated for 1 hour at 1200 °C with $SnCl_2$ showed columnar grain structures mostly. Grainith deeper cupping, a depression in the middle of Nb_3Sn grains at Nb_3Sn-Nb interface, see Fig. 7(a) were also present. Grains appeared to be elongated next to grain boundaries (GB) towards the substrate niobium in several locations. Following the first overcoat for one hour, see Fig. 7(b), new smaller grains were observed next to the intersection of Nb_3Sn GB and the substrate niobium. Locations where no additional grains formed mostly show cupping at the Nb_3Sn-Nb interface. Similar observations were made from the sample subjected to plus one-hour overcoat as shown in Figure 7(c). The next overcoat for 3 hours resulted in more grains at the interface with cupping in larger grains, Fig. 7(d). The EBSD cross-section obtained after an additional 12 hours of overcoat, Figure 7(e), shows smaller grains at the interface and/or cupping of grains. In some areas two layers of smaller grains (marked with black rectangle) were seen. An EBSD image from 60 hours overcoat is shown in Fig. 7(f). The longest coating resulted in large columnar grains traversing the thickness of Nb_3Sn layer. At Nb_3Sn-Nb interface, small triangular Nb_3Sn grains were observed in between these columnar grains at the end of grain boundaries. Most of the grains including smaller grains had depressions at the center at Nb_3Sn-Nb interface away from grain boundaries.

EBSD and XPS data suggested that the overcoat did not result in a new Nb_3Sn layer either below or above the existing one. The grains grew axially and laterally during each overcoat. Smaller grains occasionally observed at the Nb-Nb_3Sn interface in single-coat sample appeared frequently in overcoat sample indicating additional grain formation as shown in Fig. 7.b. Note that smaller grains had almost always formed at the end of Nb_3Sn grain boundaries next to Nb substrate, and they are comparatively smaller than columnar grains seen in single-coat sample. Furthermore, grain growth appeared faster next to Nb_3Sn grain boundaries where it intersects the substrate niobium. This can be seen as "cupping" at the base of many Nb_3Sn grains as shown in Fig. 7. The appearance at the interface seems consistent with the concentration contour suggested by [14]. According to [15], an excess of diffusing atoms may build up in the vicinity of grain boundaries of polycrystalline compound layers, adjacent to the other phase resulting in uneven interface. It indicates grain boundaries are the Sn transporting channels to the interface, where coating growth proceeds. These observations strongly suggest that grain boundary diffusion primarily controls the growth process.

Nb_3Sn layer thicknesses were estimated from the XPS depth profile data and several EBSD images obtained from representative overcoat sample from each experiment. Some discrepancy between the two measurements is expected because of the surface and interface roughness which may preserved throughout the sputter profile. Additionally, sputtering itself can induce roughness. Compared to XPS and EBSD, thickness estimation from optical images is assumed to be most accurate as it allows

direct examination of cross-sections. Optical micrographs were further captured from each cross-section for comparison. Estimated coating thickness as a function of coating time is shown in Figure 8. It shows non parabolic relationship between coating thickness and coating time, equation 2,

$$y = (2.48 \pm 0.10)t^{0.40 \pm 0.02} \quad (2)$$

where y and t are layer thickness (µm) and total coating time (hour) respectively.
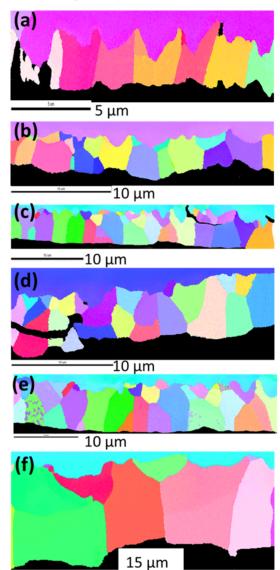

Figure 7: Cross-sectional EBSD images from top to bottom follows sequential overcoat samples. Different colors here refer to different crystallographic orientations. Nb_3Sn grains are significantly smaller compared to Nb grain, which is represented by single color on top of each image. The black regions within the Nb_3Sn layer were likely to be crack produced during the specimen preparation.

Figure 8: Variation of thin film thickness with coating time.

Past studies have also shown that Nb$_3$Sn layers grown via vapor diffusion process, does not follow a parabolic relationship ($y \propto t^{0.5}$) between the coating thickness (y) and the deposition duration (t) [16]. Non-parabolic dependence indicates that the growth process is not purely diffusion-controlled [17]. The deviation from parabolic growth was often explained by the influence of the grain boundaries, e.g., [18, 19]. Other researchers at the same time proposed alternate interpretations, e.g., "*solution-deposition*" mechanism for non-parabolic growth exponent [20, 21]. Note that if the growth is controlled via bulk diffusion or GB diffusion, it is expected have parabolic dependency between the thickness and the coating time.

Coating thickness obtained from 1-6 hour of coating (first four data points) was compared with that obtained from 3 - 78 hours coating (last four data points) in Fig. 9. Obtained growth exponent, (0.49 ±0.09) show a parabolic relationship between the layer thickness and coating time for shorter coating up to 6 hours. The growth exponent reduced to (0.37 ±0.02) for relatively longer coating of 3-78 hours. It indicates that coating growth is diffusion controlled at the beginning, and deviates from it with longer coating. It is speculated that with higher density of grain boundaries (small Nb$_3$Sn grains) and thinner coating (short diffusion length) at the beginning, supplied tin maintains the natural growth rate at Nb-Nb$_3$Sn interface via bulk or grain boundary diffusion. The growth rate reduces with longer coating because of reduced GB density (larger grains) and thicker coating (longer diffusion length) coating. It has been reported that bulk diffusion in Nb$_3$Sn gets frozen and GB diffusion dominates for longer coating [22].

Estimated coating thickness dependence on time from Fig. 5 was compared with similar measurements reported from Wuppertal University [16] in a log-log plot in Fig. 10. The growth exponent (0.40) was close to the one reported by Wuppertal (0.38), but the coefficient (specific growth rate at t=0) was higher in our case. [Note that the actual Wuppertal data from [23] appears to have growth exponent of 0.36 instead of 0.38]. The higher specific growth rate, pre-factors (2.50 vs 1.377) measured in present

experiments is attributed to a higher coating temperature of 1200 °C compared to the Wuppertal data obtained on samples coated mainly at 1160 °C.
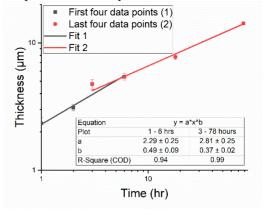

Figure 9: Growth kinetics observed in single-coat and overcoat samples. Two straight lines here represent growth kinetics for coating time of 1-6 hours and 6-78 hours.
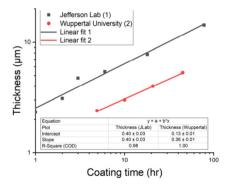

Figure 10: Growth kinetics observed in single-coat and overcoat samples compared to Wuppertal data [16].

It is normally expected that the coating growth rate k follows an Arrhenius dependency on temperature [24-25]:

$$\ln k = -\frac{Q}{RT} + C \quad (3)$$

where Q and R are activation energy and ideal gas constant respectively, and C is a constant. The dependency of coating thickness on time may be expressed as,

$$y = k(T)\, t^n \quad (4)$$

where y is the thickness of coating. Here the reported value for n greatly varied between 0 to 1 for Nb$_3$Sn growth for different preparation methods [26]. For n=0.5, the layer thickness has a parabolic time dependence as is expected for pure bulk diffusion. Parabolic time dependency exists also for the coating growth via grain boundary diffusion through a fixed array of grain boundaries [27]. Reported values of grain boundary diffusivity of tin in Nb$_3$Sn up to 800 °C are several orders higher compared to bulk diffusivity [26].

The present data shows a similar power law dependency for both the average grain size, Fig. 6, and coating thickness, Fig. 8. With substantial increase in grain size,

the number of diffusion paths is reduced, depleting the tin supply at the growth interface. The length of diffusion path also gets longer following increased thickness of the coating.

Average grain size comparison before and after the overcoat experiment, reported before, showed that the grain growth rate varied inversely with pre-overcoated grain size supporting faster growth with higher density of grain boundaries [28]. Farrel et al. [18] had proposed a relation between layer thickness and the grain growth exponent for appreciable growth in grain size:

$$z = \beta(T)t^{0.5(1-m)} \qquad (5)$$

where m and z are grain growth exponent and layer thickness respectively. $\beta(T)$ is temperature dependent prefactor. For m ~ 0.34, equation (7) gives $y \propto t^{0.33}$, which is slightly different what we obtained experimentally. Within the framework of grain boundary diffusion model, it is possible to understand the commonly observed patchy regions.

Patchy regions are thin regions of few tens to few hundreds of nanometer thickness compared to 2-3 µm thickness of regular coating. They affect RF performance adversely. EBSD analysis shows that patchy regions are composed of monocrystalline Nb_3Sn [29] as shown in Fig. 11, where larger single-colored regions were patchy areas when examined with SEM. Patchy regions are clearly deprived of GB's to facilitate Sn-flux to the growth interface underneath. As discussed above, the coating growth is significantly hindered, so the patchy area, once it forms, grows much slower than regular. The origin of patchy regions is yet all understood. Our observations in several experiment indicates that the patchy regions likely to form because of

- Poor nucleation as indicated by Fig. 5.
- Significantly low tin evaporation. i.e., low flux of tin [13].
- Farther distance from the tin or tin source, e.g., without secondary tin source the patchy region was found in the witness sample at top unlike sample at the bottom [30].
- Out-of-sight area, e.g., cutout study of Nb_3Sn coated cavity showed comparatively higher coverage of patches in equator compared to cavity region [31].

One possible reason for the formation of patchy regions could be the higher sticking coefficient and lower surface ad-atom mobility during the nucleation stage, which may result in out-of-sight or farther areas to remain poorly covered with tin. Once the process progresses to growth stage, such areas may present large bare niobium areas to arriving tin atoms with higher mobility at this stage. Due to the absence of pre-nucleated centers and high tin mobility, such areas will promote the growth of large single crystal grains, i.e., the patchy areas. Note that there are some studies which also showed some link with substrate orientations, which may also link with

mobility and sticking phenomenon. More discussions are available in [31-32].

RF PROPERTIES

Several other thin film deposition techniques are in progress, but they have yet to be able to produce promising Nb_3Sn RF cavities. Nb_3Sn thin films prepared by vapour diffusion process is presently leading the RF application. Notable Nb_3Sn coated SRF cavities were produced at Wuppertal University three decades ago, which resulted in low field quality factors of 2×10^{10} at 4 K and 1×10^{11} at 2 K, tested at JLab. Despite promising quality factor and accelerating gradient, cavities suffered precipitous Q-slope, also known as *"Wuppertal slope"* with increasing field. Reproducible Q-slope at that time was assumed to be fundamental as the Q-slope onset was near the lower critical magnetic field of Nb_3Sn. Similar sharp Q-slopes were later reproduced in multiple Nb_3Sn cavities produced at Cornell University, Jefferson Lab and Fermilab at early stages of their Nb_3Sn programs following the revival of Nb_3Sn for SRF cavities in 2009. It has been then demonstrated that the Q-slope is not fundamental, and several Q-slope free cavities were produced [33]. Wuppertal-like slope still appears with slight deviation in coating parameters. The origin of Wuppertal slope is not fully established yet.
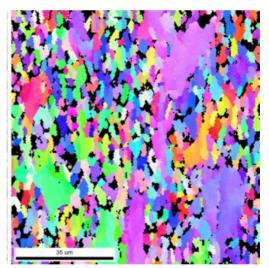
Figure 11: EBSD image obtained from sample with patchy regions. Here single colored large areas appear patchy in SEM image [29].

JLab coating followed the Siemens configuration with a single heater and active pumping during the coating, and early cavities consistently suffered Q-slope similar to Wuppertal cavities. Following the demonstration of Q-slope removal at Cornell University, samples prepared at the Jefferson lab coating facility and Cornell University were compared by analyzing them with several material characterization techniques. Microstructure, composition and topography were found very similar for each sample. SIMS analysis on the other hand showed higher presence of titanium throughout the Nb_3Sn layer in JLab coated sample compared to sample obtained from Cornell [34].

Titanium was likely derived from TIG welds present in the sample chamber. Since cavities coated before, which had Q-slope, had NbTi flanges, we suspected Ti contamination during the coating. Molybdenum hardware, white at the beginning, used during the coating of those cavities were found to develop purple color afterward. EDS examination showed Ti on those parts corroborating titanium contamination speculation in coated cavities. Note that Ti foils were used as gettering material to maintain the purity of niobium during the Nb_3Sn coating at Wuppertal [35]. It is also known that Ti can affect field dependence in niobium cavities [36-37]. Under assumption that Ti is likely the cause of Q-slope in Nb_3Sn cavities, Ti contamination was avoided to the extent possible following the coating system upgrade in 2017.

Production of an almost Q-slope free Nb_3Sn single-cell cavity was produced for the first time, but the Q was below 1×10^{10} at 2 K [30]. Several cavities were coated later including witness samples. Several cavities still suffered Q-slopes to a different extent. Inspection of cavities and analysis of witness samples linked observed Q-slope to

- Macroscopic surface defects in the substrate
- Condensation of tin residue at the surface
- Non-uniform coating with probable patchy regions

During the coating of 5-cell cavities, it had been observed that non-uniform coating limits the quality factor and the accelerating gradient. New cavities with no surface defects were added to Nb_3Sn program. The coating process was then modified to eliminate possible residual tin condensation and non-uniformity. Two-cavity setup was implemented, where the cavity of interest was positioned at the bottom close to the tin source. Another dummy cavity was placed on top and a temperature gradient of ~ 85 °C between the top (cold) and bottom (hot) of paired cavity setup. It was expected that any residual tin would condense on the cavity at the top position. A secondary tin source was employed to increase tin flux and to avoid patchy regions by facilitating a uniform coating. RDT7 and RDT10 were coated uniformly before, but tin residues were seen in witness samples, and the cavities suffered from a strong Q-slope. Same cavities were coated later by coupling with another dummy cavity in two-cavity setups. Almost Q-slope free results were achieved as shown in Figure 12. The measured value of low field Q_0 was 3×10^{10} at 4 K and 1×10^{11} at 2 K without a significant Q-slope. The cavity maintained a Q_0 of ~ 2×10^{10} at 4 K and > 3×10^{10} at 2 K before quench at >15 MV/m. Further details on cavity coatings are available in [38].

SUMMARY

Samples representing different stages of Nb_3Sn formation have been produced and examined to elicit the effects of nucleation, growth, process conditions, and impurities. Nb_3Sn films from few hundreds of nm up to ~15 μm were grown and characterized using different material characterization techniques. Nucleation yields two tin forms. Three-dimension particles are visible to in SEM, and a two-dimensional form no thicker than a few

atomic layers, which are evident to XPS, SAM and analytical TEM-EDS. Following the nucleation step, a layer of Nb_3Sn forms readily with a rapid temperature ramp. Tin primarily diffuses downward through grain boundaries to the Nb_3Sn-Nb interface, resulting in growth of Nb_3Sn that extends into the Nb bulk. Grain size and thickness both had a power law dependency on total coating time. The lateral grain growth rate is slower than thickness growth rate. Non-parabolic growth dependence is consistent with significant grain growth, which is superimposed on GB diffusion. Patchy regions in Nb_3Sn coating are large single crystalline grains, which are a significantly thinner coating because of the few grain boundaries available for tin transport. Nb_3Sn coating layers produced after overcoats are similar to the continuous layer obtained in single-coat. We modified the cavity coating process to eliminate possible candidates responsible for Q-slope. The best coated cavity had a Q_0 of ~ 2×10^{10} at 4 K and > 3×10^{10} at 2 K before quench at >15 MV/m.
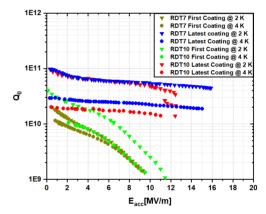

Figure 12: Comparison of latest RF test results from RDT10 and RDT7 with those after their first coating. RDT10 is expected to have higher Q_0 at 4 K than presented here as we expect losses on the flanges because of shorter beam pipes.

REFERENCES

[1] B.T. Matthias, T.H. Geballe, S. Geller and E. Corenzwit,. "Superconductivity of Nb3Sn." *Physical Review*, vol. 95(6), p.1435, 1954.

[2] M.K. Transtrum, G. Catelani, and J.P. Sethna, "Superheating field of superconductors within Ginzburg-Landau theory." *Physical Review B*, vol. 83(9), p.094505, 2011.

[3] G. Arnolds, and D. Proch, "Measurement on a Nb3Sn structure for linear accelerator application." *IEEE Transactions on Magnetics*, vol. 13(1), pp.500-503, 1977.

[4] P. Kneisel, O. Stoltz and J. Halbritter, "Measurements of superconducting Nb3Sn cavities in the GHz range." *IEEE Transactions on Magnetics*, vol. 15(1), pp.21-24, 1979.

[5] G. Müller, R. Roeth, H. Piel, D. Mansen, J. Pouryamout and P. Kneisel, "Nb3Sn layers on high purity Nb cavities with very high quality factors and accelerating gradients," in *Proc. EPAC'96*, Barcelona, Spain, Jun. 1996, pp. 2085-2087.

[6] R. D. Porter *et al.,* "Next Generation Nb3Sn SRF Cavities for Linear Accelerators", in *Proc. 29th Linear Accelerator Conf. (LINAC'18)*, Beijing, China, Sep. 2018, pp. 462-465.

[7] S. Posen *et al.,* Development of Nb3Sn Coatings for Superconducting RF Cavities at Fermilab. No. FERMILAB-CONF-18-477-TD. Fermi National Accelerator Lab. (FNAL), Batavia, IL (United States), 2018.

[8] G. V. Eremeev, M. J. Kelley, C. E. Reece, U. Pudasaini and J. Tuggle, "Progress With Multi-Cell Nb3Sn Cavity Development Linked With Sample Materials Characterization", in *Proc. 17th Int. Conf. RF Superconductivity (SRF'15)*, Whistler, Canada, Sep. 2015, paper TUBA05, pp. 505-511.

[9] Z. Q. Yang, Y. He, and F. Pan, "Several Experimental Phenomena of Sn Nucleation on Nb Surface Observed at IMP", in *Proc. 29th Linear Accelerator Conf. (LINAC'18)*, Beijing, China, Sep. 2018, pp. 412-416. doi:10.18429/JACoW-LINAC2018-TUPO038

[10] J.P. Charlesworth, I. Macphail and P.E. Madsen, "Experimental work on the niobium-tin constitution diagram and related studies." *Journal of Materials Science, vol. 5(7)*, pp.580-603, 1970.

[11] E. Saur, and J. Wurm, "Präparation und Supraleitungseigenschaften von Niobdrahtproben mit Nb3Sn-Überzug." *Naturwissenschaften,* vol. 49(6), pp.127-128, 1962.

[12] Uttar Pudasaini *et al*. *Supercond. Sci. Technol*. vol. 32, pp. 045008, 2019.

[13] U. Pudasaini, M. J. Kelley, G. V. Eremeev, C. E. Reece, and J. Tuggle, "Surface Studies of Nb3Sn Coated Samples Prepared under Different Coating Conditions", *in Proc. 18th Int. Conf. RF Superconductivity (SRF'17)*, Lanzhou, China, Jul. 2017, pp. 894-899. doi:10.18429/JACoW-SRF2017-THPB069

[14] J. D. Baird, "The formation of intermediate alloy layers in the inter-diffusion of metals," *Journal of Nuclear Energy. Part A.Reactor Science,* vol. 11 *(2-4),* pp. 81-88, 1960.

[15] V. I. Dybkov, *Reaction diffusion and solid state chemical kinetics: handbook*. Trans Tech Publ., 2010.

[16] M. Peiniger *et al*, "'Work on Nb3Sn cavities at Wuppertal;" *Third workshop on RF (radiofrequency) superconductivity*, No. ANL-PHY--88-1-VOL. 2. 1988.

[17] A. Paul and S. Divinski, *Handbook of Solid State Diffusion: Volume 1: Diffusion Fundamentals and Techniques*. vol. 1. Elsevier, 2017.

[18] H. H. Farrell, G. H. Gilmer and M. Suenaga, "Grain boundary diffusion and growth of intermetallic layers: Nb3Sn," *J. Appl. Phys.,* vol. 45, *(9),* pp. 4025-4035, 1974.

[19] H. H. Farrell, G. H. Gilmer and M. Suenaga, "Diffusion mechanisms for the growth of Nb3Sn intermetallic layers," *Thin Solid Films,* vol. 25, (1), pp. 253-264, 1975.

[20] G. N. Ronami *et al*, "Investigation of diffusion in the Nb-Sn system," *Izvestiya Akademii Nauk SSSR, Neorganicheskie Materialy,* vol. 7, *(9),* pp. 1490-1493, 1971.

[21] C. F. Old and I. Macphall, "The mechanism and kinetics of growth of the superconducting compound Nb3Sn," *J. Mater. Sci.,* vol. 4, *(3),* pp. 202-207, 1969.

[22] X. Xu, "A review and prospects for Nb3Sn superconductor development," *Superconductor Science and Technology,* vol. 30, *(9),* pp. 093001, 2017.

[23] Jun Ding, "Herstellung Und Untersuchung Supraleitender Nb3Sn-Schichten in Mehrzelligen 3- GHz-Beschleunigungsresonatoren", Wuppertal University, 1986.

[24] R. H. Parker, *"An Introduction to Chemical Metallurgy: International Series on Materials Science and Technology"*. Vol. 26, Elsevier, 2016.

[25] A. K. Kumar and A. Paul, "Interdiffusion and growth of the superconductor Nb3Sn in Nb/Cu (Sn) diffusion couples," *J Electron Mater,* vol. 38, *(5),* pp. 700-705, 2009.

[26] H. Müller and T. Schneider, "Heat treatment of Nb3Sn conductors," *Cryogenics,* vol. 48, *(7-8),* pp. 323-330, 2008.

[27] S. Foner and B. B. Schwartz, *Superconductor Materials Science: Metallurgy, Fabrication and Applications*, Springer Science & Business Media, 2012.

[28] U. Pudasaini, M. J. Kelley, G. V. Eremeev, C. E. Reece, and J. Tuggle, "Insights into Formation of Nb3Sn Film During the Vapor Diffusion Process", in *Proc. 18th Int. Conf. RF Superconductivity (SRF'17)*, Lanzhou, China, Jul. 2017, pp. 539-542. doi:10.18429/JACoW-SRF2017-TUPB067

[29] J. Tuggle *et al*, "Electron Backscatter Diffraction of Nb3Sn Coated Niobium: revealing Structure as a Function of Depth" *Journal of Vacuum Science & Technology B,* Accepted, 2019.

[30] U. Pudasaini *et al.*, "Nb3Sn Multicell Cavity Coating at JLab", in *Proc. 9th Int. Particle Accelerator Conf. (IPAC'18)*, Vancouver, Canada, Apr.-May 2018, pp. 1798-1803. doi:10.18429/JACoW-IPAC2018-WEYGBF3

[31] U. Pudasaini *et al*., "Analysis of RF loss and material composition of C3C4 cavity cutouts" JLab TechNote JLAB-TN-19-024, 2019.

[32] U. Pudasaini *et al*., "Growth of Nb3Sn coating in vapor diffusion process" to be published.

[33] S. Posen and M. Liepe, Advances in development of Nb 3 Sn superconducting radio-frequency cavities, *Physical Review Special Topics-Accelerators and Beams*, vol. 17(11), p.112001, 2014.

[34] J. Tuggle *et al.,* "Secondary ion mass spectrometry for superconducting radiofrequency cavity materials." *Journal of Vacuum Science & Technology B, Nanotechnology and Microelectronics: Materials, Processing, Measurement, and Phenomena, vol.* 36.5, pp. 052907, 2018.

[35] M. Peiniger, PhD dissertation, Wuppertal University, 1989.

[36] P. Dhakal, *et al.,* "Effect of high temperature heat treatments on the quality factor of a large-grain superconducting radio-frequency niobium cavity." *Physical Review Special Topics-Accelerators and Beams*, vol. 16.4, pp. 042001, 2013.

[37] J. Knobloch, PhD dissertation, Cornell University, 1997.

[38] U. Pudasaini *et al.*, "Recent results from Nb3Sn single cell cavities coated at Jefferson Lab", *in Proc. 19th Int. Conf. RF Superconductivity (SRF'19)*, Hamburg, Germany, Jun.-Jul. 2019, paper MOP018.